Acta Pharm. **76** (2026) 260006
https://doi.org/10.2478/acph-2026-0006

Short communication

The effect of astragaloside IV on a model of isoproterenol--induced hypertrophic injury in H9c2 cells

YANG LONG[1]
YUAN XIAO[1]
CHUN CHEN[2]
CHAO PENG[3]
YUXI ZHANG[4,*]

[1] *Department of Pharmacy Xing Yi People's Hospital Xing Yi, 562499, P.R. China*

[2] *Orthopedic Joint Surgery Xing Yi People's Hospital Xing Yi, 562499, P.R. China*

[3] *Cardiovascular Medicine Department, Xing Yi People's Hospital, Xing Yi, 562499 P.R. China*

[4] *Affiliated Hospital of Sichuan Nursing Vocational College (The Third People's Hospital of Sichuan Province), Chengdu City SiChuan Province, 610100 P.R. China*

Accepted January 13, 2026
Published online January 16, 2026

ABSTRACT

The objective of this study was to explore the protective effect of astragaloside IV on a model of isoproterenol-induced (ISO) hypertrophic injury in rat cardiomyocytes H9c2 (cell line derived from embryonic BD1X rat heart tissue). A cell hypertrophy injury model was established (H9c2 cells treated with 100 μmol L^{-1} ISO). The cells were divided into normal control, a model group, and an astragaloside IV group at several concentrations. Astragaloside IV was pre-administered for 2 hours, followed by ISO treatment for 24 hours. Cell viability, cell surface area, apoptosis rate, lactate dehydrogenase (LDH) activity, reactive oxygen species (ROS), superoxide dismutase (SOD), the mRNA levels of Bcl-2, Bax, p62, and LC3, the protein expressions of Sirt1, p62, caspase-3, beclin, and p53 and the LC3II/LC3I ratio were detected. Astragaloside IV significantly alleviated ISO-induced hypertrophy injury in H9c2 cells, reduced cell surface area and LDH release, decreased apoptosis rate and intracellular ROS levels, increased SOD levels, upregulated the expressions of autophagy-related mRNA and proteins, and downregulated the expressions of apoptosis-related mRNA and proteins. Astragaloside IV can effectively inhibit ISO-induced hypertrophy and apoptosis in H9c2 cells, and its mechanism may be related to promoting autophagy and reducing oxidative stress.

Keywords: astragaloside IV, cardiac hypertrophy, apoptosis, autophagy, oxidative stress

INTRODUCTION

Pathological myocardial hypertrophy (MH) is an adaptive compensatory response of the heart to various stimuli, resulting in an increase in the volume and mass of myocardial cells (1–3). It is a common physiological phenomenon in the early stage of various cardiovascular diseases, including hypertension, myocardial infarction or ischemia, atherosclerosis, *etc.* If external intervention is lacking for a long time, this adaptive compensatory response will be decompensated when it exceeds a certain limit, causing myocardial dysfunction and eventually developing into heart failure (HF) (4–6). At present, the main therapeutic drugs for MH are angiotensin-converting enzyme inhibitors, beta-blockers, *etc.* Although they have improved the clinical symptoms of patients to a certain extent, they still cannot significantly reduce the mortality rate (7–9).

* Correspondence; e-mail: yaoshanshiliao@xingyihospital.top

Astragaloside IV is the main component of the traditional Chinese medicine *Astragalus membranaceus*. Recent studies have proved that astragaloside IV can act as a scavenger of endogenous reactive oxygen species (ROS) (10), as it exerts antioxidant and anti-inflammatory effects and is involved in autophagy activation (11). Astragaloside IV has been proven to alleviate cardiovascular diseases, such as hypertension and myocardial infarction (12). Since ROS and autophagy play a key role in cardiac hypertrophy, the author speculates that astragaloside IV may exert antioxidant effects and induce autophagy by eliminating ROS and damaged mitochondria, thereby preventing the development of cardiac hypertrophy and the occurrence of heart failure. For this purpose, in this study, isoproterenol (ISO) is selected to induce hypertrophic injury in H9c2 cells, and the effect of astragaloside IV on ISO-induced hypertrophic cardiomyocytes as a model of hypertrophic injury is observed.

Bcl-2 can alleviate apoptosis by reducing the production of ROS, whereas Bax can change mitochondrial membrane permeability and promote the release of cytochrome c by inhibiting Bcl-2 as an antiapoptotic factor, thereby inducing caspase activation and cell death (13, 14). Protein p53 is a transcription factor and is regarded as an indicator of apoptosis (15, 16). To further verify the protective effect of astragaloside IV on apoptosis, the expressions of Bcl-2, Bax mRNA and p53 were detected in this experiment.

LC3I can be transformed into LC3II. Ratio of LC3II/LC3I is a biomarker, reflecting the degree of autophagy. As one of the marker proteins reflecting autophagic activity, the content of p62 indirectly reflects the clearance level of autophagosomes. To further explore the protective mechanism of astragaloside IV on myocardial hypertrophy, the expressions of autophagy-related proteins (beclin, p62, LC3I, LC3II, Sirtl) were followed by Western blot in this experiment. Through the above experiments, the protective mechanism of astragaloside IV against myocardial hypertrophy was further verified.

EXPERIMENTAL

Culture of H9c2 cells. – Cell line H9c2 (rat cardiomyocytes) was purchased from the cell bank of Hefei WanWu Biotechnology, China. The cells were cultured at 5 % CO_2 at 37 °C using DMEM medium (Thermo Fisher Scientific, USA) containing 10 % fetal bovine serum. When the cell density reached approximately 80 %, digestion and passage were carried out. Cells in the logarithmic growth phase and in good condition were taken for subsequent experiments.

Experimental grouping. – H9c2 cardiomyocytes were divided into 5 groups, and each group was treated with normal medium containing 1 % fetal bovine serum. The normal control group (received no treatment at all), the model group (ISO (Item No. 51-30-9, Med Chem Express, USA) in a final concentration of 100 μmol L^{-1} was added and cultured for 24 hours), and three astragaloside IV groups (pretreated with astragaloside IV at final concentrations of 6.08, 12.16 and 24 μmol L^{-1} for 2 h respectively, and then cultured with 100 μmol L^{-1} ISO for 24 h).

Detection of H9c2 cell viability by the CCK-8 (Beijing Codon Biotechnology Co.) method. – H9c2 cells in the logarithmic growth phase were prepared into a cell suspension and inoculated in a 96-well plate (cell culture plates, Corning Corporation, USA) for 24 hours.

Then, 1 % fetal bovine serum medium was used for overnight culture. Different concentrations of astragaloside IV (1.56, 3.13, 6.08, 12.16, 24, 50, 100, and 200 μmol L^{-1}) were added to the administration groups for 2 hours, then cultured with 100 μmol L^{-1} ISO for 24 hours, and later 810 μL of CCK-reagent was added to each well for continued culture for 2 hours. Finally, the optical density (*D*) of each well at λ = 450 nm were detected, and the cellular proliferation inhibition rate was calculated using Equation *1*.

$$\text{Proliferation inhibition rate (\%)} = \frac{D_{\text{exper. group}} - D_{\text{blank group}}}{D_{\text{neg. control group}} - D_{\text{blank group}}} \times 100 \quad (1)$$

Cell surface area staining. – After the cells were grouped and treated, they were fixed in 4 % paraformaldehyde, rinsed with PBS (Thermo Fisher Scientific) three times, and then sealed in PBS solution (containing 1 % BSA) for 60 minutes at room temperature. TRITC--Phalloidin (Xi'an Qiyue Biology) with a final concentration of 5 mg L^{-1} was added for light-protected staining for 30 minutes, and PBS was used for washing three times. DAPI was added to stain the cell nuclei in the dark for 5 minutes, and washed three times with PBS. The cytoskeletal microfilaments of myocardial cells were observed under a fluorescence microscope. Ten fields of view were randomly selected from each group, and the surface area of H9c2 cells was determined by Image J2 (National Institutes of Health, USA).

Lactate dehydrogenase (LDH), ROS and superoxide dismutase (SOD) assays. – After the cells were grouped and treated, the contents of LDH (Yeasen Biotechnology, China), ROS and SOD (Shanghai Enzyme-linked Biotechnology, China) in the cells were determined according to the instructions of the detection kits, and using the Epoch2 microplate reader (Bio-Tek Company, USA).

Detection of apoptosis by Hoechst 33342 staining. – After the cells were grouped and treated, the detection was carried out according to the instructions of the kit. The cells were fixed with 4 % paraformaldehyde for 5 min at room temperature and washed three times with PBS, stained with Hoechst 33342 in the dark for 15 min, rinsed with PBS three times to remove the staining solution, and then observed under a fluorescence microscope. The apoptosis rate of cells was calculated.

TUNEL staining. – After the cells were grouped and treated, 4 % paraformaldehyde was used to fix the cells, and TUNEL staining was performed according to the instructions of the kit (YiSheng Biotechnology, China). Observation was performed using an inverted fluorescence microscope. Ten fields of view were selected and statistically analysed using ImageJ software (National Institutes of Health).

qRT-PCR detection. – Cell grouping and intervention methods are the same as those under "Cell surface area staining". After 24 h, cells from each group were collected. The total RNA of the cells was extracted on ice according to the steps in the total RNA extraction kit (Shandong Sikejie Biotechnology, China) manual, and the RNA content and purity were detected. RNA was reverse transcribed into cDNA using a reverse transcription kit (Shandong Sikejie Biotechnology). Reverse transcription conditions: 42 °C for 15 min; 95 °C for 5 min; 72 °C for 5 min, then stored at 4 °C. Finally, a PCR reaction was carried out. The reaction system (Shandong Sikejie Biotechnology) was 20 μL, and the reaction conditions were: 95 °C for 2 min; thermal cycling at 95 °C for 15 s; annealing at 60 °C for 40 s, repeating

Table I. Primer sequence

Gene	Upstream sequence	Downstream sequence
Bcl-2	CTGTGGATGACTGAGTACC	GAGACAGCCAGGAGAAAT
Bax	ATCCAAGACCAGGGTGGCT	CCTTCCCCCATTCATCCCAG
p62	TCGTGGTCGTGGGGTGTCTG	TCTGGTGATGGAGCCTCTTACTGG
LC3	TATCCACACCCATCGCTGACA	CCTCTTGACTCAGAAGCCGAA
β-actin	TCCTGTGGCATCCACGAAACT	GAAGCATTTGCGGTGGACGAT

40 cycles. After the reaction was completed, the data was exported. *β*-actin was used as the internal reference. The relative expression levels of each gene were calculated using the relative quantification method of $2^{-\Delta\Delta Ct}$. (The primer sequences synthesised by Fuzhou Seville Biotechnology Engineering, China, Table I).

Western blot detection. – Total protein was extracted using RIPA lysis buffer (Biyun Tian Biotechnology, China) containing phenylmethylsulfonyl fluoride protease inhibitor (Biyun Tian Biotechnology). Protein concentration was measured by bicinchoninic acid method. Protein was denatured by boiling and was separated by SDS-PAGE gel electrophoresis. Transfer of proteins to the PVDF membrane was performed at 100 V for 1.5 h). Then the membrane was sealed with 5 % skimmed milk for 1.5 h at room temperature. Membranes were incubated with antibodies against Sirt1 (Shanghai Enzyme-Linked Biotechnology, China), p62 (Shanghai Enzyme-Linked Biotechnology), beclin (Aimeijie Technology, China), p53 (Shanghai Enzyme-Linked Biotechnology), caspase-3 (Cell Signaling Technology, China) and LC3 (Shanghai Lianmai Bioengineerin, China) overnight at 4 °C. Membranes were incubated with secondary antibodies (labeled with horseradish peroxidase) (diluted with Tris-buffered saline with Tween) against anti-Sirt1 (Merck, Germany), anti-p62 (Merck), anti-p53 (Merck), anti-caspase-3 (Wuhan Finn Biotechnology, China), and anti-LC3 (Fujifilm, Japan) at room temperature for 2 h. Finally, the protein signals were detected by

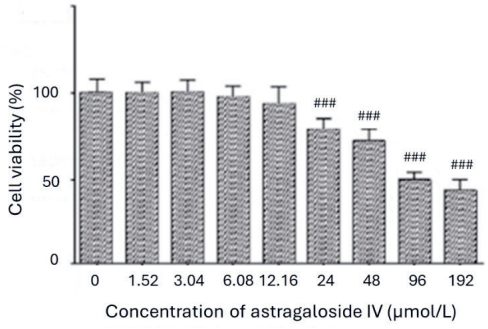

Fig. 1. The effect of astrastragaloside IV on the viability of H9c2 cells ($n = 3$). Compared with the control group (0 μmol L^{-1}), $^{###}p < 0.001$.

a chemiluminescence imaging system (Beyotime Biotechnology, China). The results were analysed with the use of ImageJ software (National Institutes of Health).

Statistical processing was conducted using SPSS22.0 software (IBM Corporation) for statistical analysis. All data were expressed as average value ± SD.

One-way ANOVA was used for the comparison among multiple groups of data with normal distribution, and Tukey's multiple comparisons test was used for multiple comparisons between groups. $p < 0.05$ was considered statistically significant.

RESULTS AND DISCUSSION

The effect of astragaloside IV on the viability of H9c2 cells is shown in Fig. 1. When the concentration is less than 24 μmol L^{-1}, astragaloside IV has no cytotoxicity to H9c2 cells. Therefore, astragaloside IV at concentrations of 6.08, 12.16, and 24 μmol L^{-1} was selected for the subsequent experiments.

The results of the effect of astragaloside IV on the surface area of H9c2 cells induced by ISO is shown in Fig. 2. Compared with the normal control group, the cell volume in the models group increased, the fluorescence of the skeletal microfilaments was brighter, the microfilament density increased, and occasionally the microfilaments aggregated into clusters, with disordered arrangement and uneven distribution. The cell surface area also significantly increased ($p < 0.001$). Compared with the model group, a decrease in the density of cytoskeletal microfilaments was observed in each group of astragaloside IV,

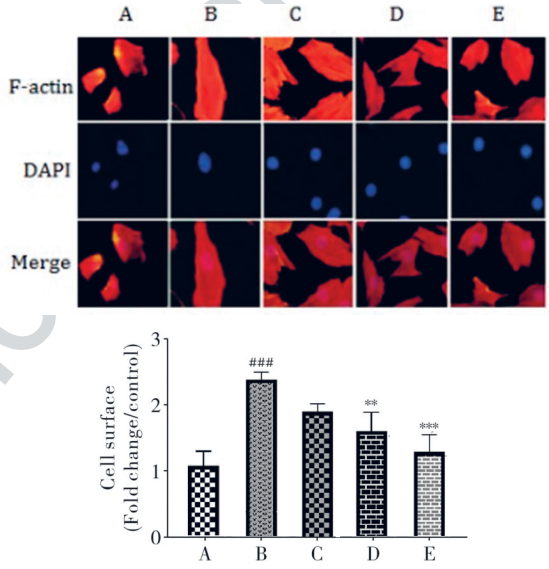

Fig. 2. Effect of astragaloside IV on the surface area of H9c2 cells induced by ISO (n = 3), (×400). A – normal control group; B – model group; C – astragaloside IV group (c = 6.08 μmol L^{-1}); D – astragaloside IV group (c = 12.16 μmol L^{-1}); E – astragaloside IV group (c = 24 μmol L^{-1}). Compared with the normal control group, $^{###}$ $p < 0.001$; compared with the model group, ** $p < 0.01$, *** $p < 0.001$.

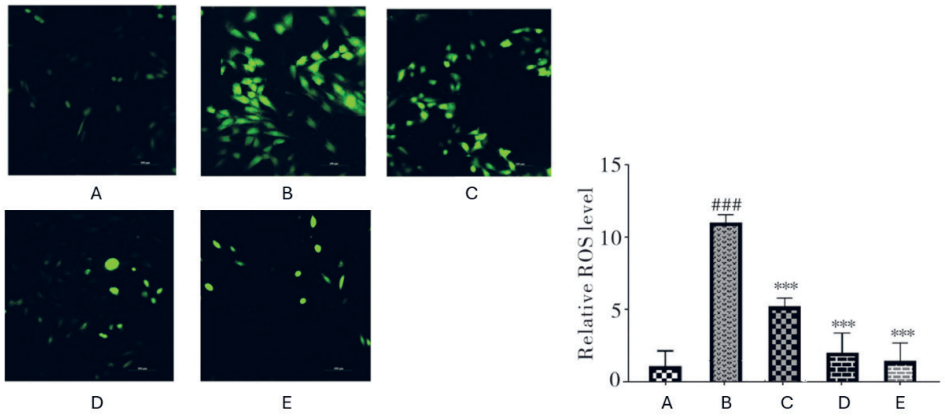

Fig. 3. The effect of astragaloside IV on ROS levels in ISO-induced H9c2 cells ($n = 3$), (×200). A – normal control group; B – model group; C – astragaloside IV group ($c = 6.08$ μmol L^{-1}); D – astragaloside IV group ($c = 12.16$ μmol L^{-1}); E – astragaloside IV group ($c = 24$ μmol L^{-1}). Compared with the normal control group, $^{###}p < 0.001$; compared with the model group, $^{***}p < 0.001$.

with a more orderly arrangement and uniform distribution. Mast cells with high fluorescence intensity were rarely seen. The cell surface area in the 12.16 and 24 μmol L^{-1} group of astragaloside IV was significantly reduced ($p = 0.008$ and $p < 0.001$).

The effect of astragaloside IV on ROS levels in ISO-induced H9c2 cells is shown in Fig. 3. Compared with the normal control group, the ROS level in the model group cells was significantly increased ($p < 0.001$). Compared with the model group, the ROS levels in the cells of each concentration group of astragaloside IV were significantly decreased ($p < 0.001$).

Effect of astragaloside IV on LDH release and SOD activity in H9c2 cells induced by ISO is presented in Fig. 4. Compared with the normal control group, the LDH level in the culture supernatant of the model group was significantly increased ($p < 0.001$), and the intracellular SOD activity was significantly decreased ($p = 0.01$). Compared with the model group, the LDH level in the culture supernatant of each concentration group of astragalo-

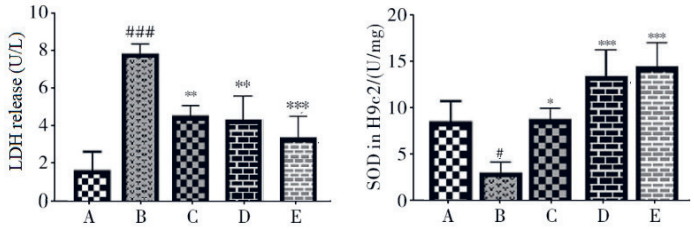

Fig. 4. The effect of astragaloside IV on LDH release and SOD activity in H9c2 cells induced by ISO (Compared with the normal control group). $n = 3$. A – normal control group; B – model group; C – astragaloside IV group ($c = 6.08$ μmol L^{-1}); D – astragaloside IV group ($c = 12.16$ μmol L^{-1}); E – astragaloside IV group ($c = 24$ μmol L^{-1}). Compared with the normal control group, $^{#}p < 0.05$ and $^{###}p < 0.001$; compared with the model group, $^{*}p < 0.05$, $^{**}p < 0.01$, $^{***}p < 0.001$.

side IV was significantly decreased, and the intracellular SOD activity was significantly increased ($p < 0.001$).

The effect of astragaloside IV on ISO-induced apoptosis of H9c2 cells is presented in Fig. 5. Hoechst 33342 staining showed that, as compared with the normal control group (the apoptosis rate: 0.9), the apoptosis rate of the model group (the apoptosis rate: 3.5) was significantly increased ($p < 0.001$). As compared with the model group (the apoptosis rate: 3.5), the apoptosis rate of cells in each concentration group of astragaloside IV (the apoptosis rates were 2.2, 2.0, and 1.9 in different concentration groups) was significantly decrease ($p < 0.01$, $p < 0.001$, and $p < 0.001$, respectively). The results of TUNEL staining showed that, as compared with the normal control group (the apoptosis rate: 0.9), the apoptosis rate of the model group (the apoptosis rate: 3.8) was significantly increased ($p < 0.001$) (Fig. 6). As compared with the model group (the apoptosis rate: 3.8), the apoptosis rate of cells in each concentration group of astragaloside IV (the apoptosis rates were 3.0, 2.9, and 1.8 in different concentration groups) was significantly decreased ($p < 0.001$ for all three astragaloside IV concentrations).

The effect of astragaloside IV on the mRNA expressions of Bcl-2, Bax, p62 and LC3 in H9c2 cells induced by ISO is shown in Fig. 7. Compared with the normal control group, mRNA expressions of Bax and p62 in the model group cells were significantly increased, while the mRNA expressions of Bcl-2 and LC3 were significantly decreased ($p = 0.03$ or

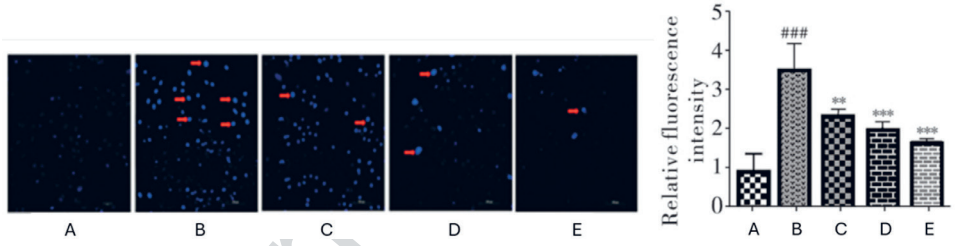

Fig. 5. Hoechst 33342 staining to detect the effect of astragaloside IV on ISO-induced apoptosis of H9c2 cells ($n = 3$), (×200). A – normal control group; B – model group; C – astragaloside IV group ($c = 6.08$ μmol L^{-1}); D – astragaloside IV group ($c = 12.16$ μmol L^{-1}); E – astragaloside IV group ($c = 24$ μmol L^{-1}). Compared with the normal control group, $^{###}p < 0.001$; compared with the model group, $^{**}p < 0.01$, $^{***}p < 0.001$.

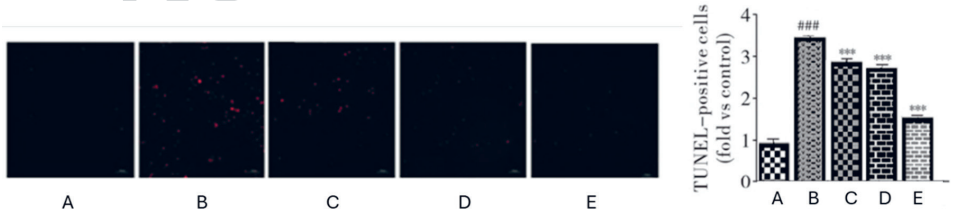

Fig. 6. TUNEL staining for the effect of astragaloside IV on ISO-induced apoptosis of H9c2 cells ($n = 3$), (×100). A – normal control group; B – model group; C – astragaloside IV group ($c = 6.08$ μmol L^{-1}); D – astragaloside IV group ($c = 12.16$ μmol L^{-1}); E – astragaloside IV group ($c = 24$ μmol L^{-1}). Compared with the normal control group, $^{###}p < 0.001$; compared with the model group, $^{***}p < 0.001$.

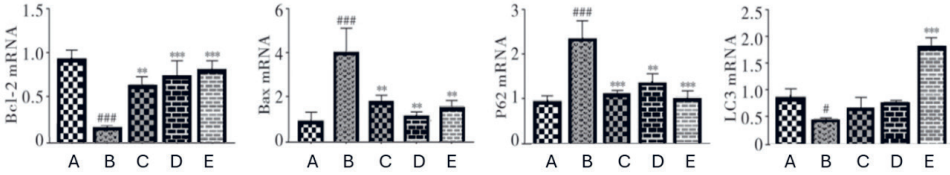

Fig. 7. The effect of astragaloside IV on the mRNA expressions of Bcl-2, Bax, p62 and LC3 in H9c2 cells induced by ISO ($n = 4$), using β-actin as the internal reference gene, the relative expression level of the target gene was calculated by the $2^{-\Delta\Delta Ct}$ method ($n = 3$). A – normal control group; B – model group; C – astragaloside IV group ($c = 6.08$ μmol L^{-1}); D – astragaloside IV group ($c = 12.16$ μmol L^{-1}); E – astragaloside IV group ($c = 24$ μmol L^{-1}). Compared with the normal control group, $^{\#}p < 0.05$, $^{\#\#\#}p < 0.001$; compared with the model group, $^{**}p < 0.01$, $^{***}p < 0.001$.

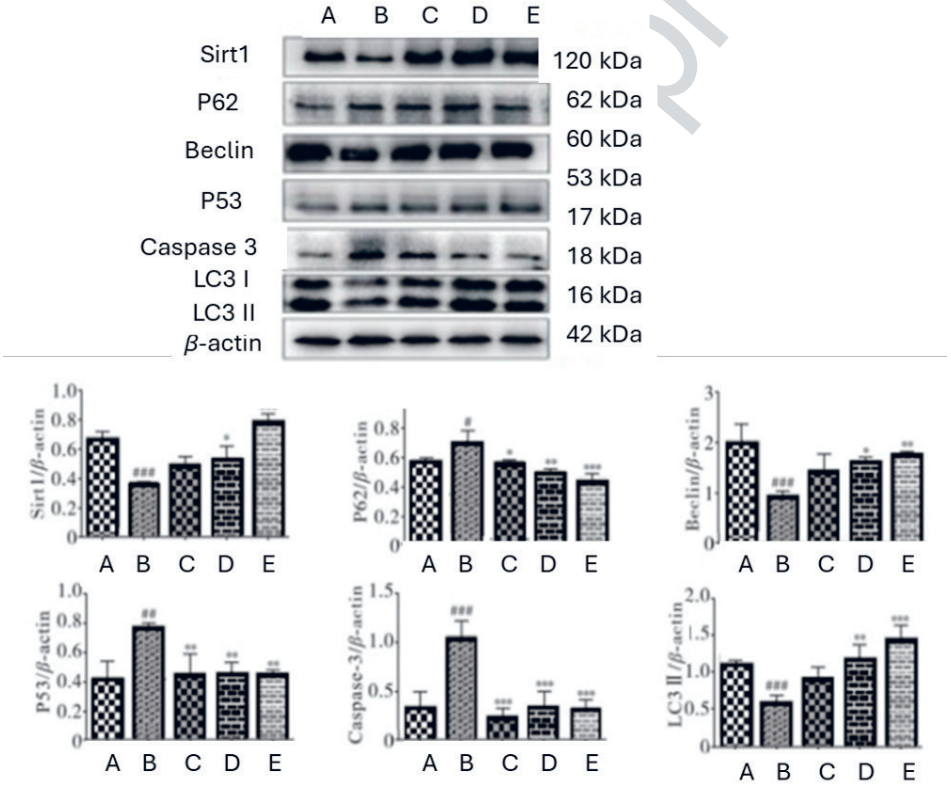

Fig. 8. The effect of astragaloside IV on the protein expressions of LC3, beclin, Sirt1, p53, p62 and caspase-3 in H9c2 cells induced by ISO ($n = 3$). A – normal control group; B – model group; C – astragaloside IV group ($c = 6.08$ μmol L^{-1}); D – astragaloside IV group ($c = 12.16$ μmol L^{-1}); E – astragaloside IV group ($c = 24$ μmol L^{-1}). Compared with the normal control group, $^{\#}p < 0.05$, $^{\#\#}p < 0.01$, $^{\#\#\#}p < 0.001$; compared with the model group, $^{*}p > < 0.05$, $^{**}p < 0.01$, $^{***}p < 0.001$.

$p < 0.001$). Compared with the model group, except that there was no statistically significant difference in the expression of LC3 mRNA in the 6.08 and 12.16 μmol L^{-1} groups of astragaloside IV ($p > 0.05$), the expressions of Bax and p62 mRNA in the cells of each concentration group of astragaloside IV were significantly decreased, and the expressions of Bcl-2 and LC3 were significantly increased ($p < 0.01$ or $p < 0.001$).

The effects of astragaloside IV on the protein expressions of LC3, beclin, Sirt1, p53, p62 and caspase-3 in H9c2 cells induced by ISO are presented in Fig. 8. Compared with the normal control group, the protein expression of beclin, Sirt1 and LC3II in the model group were significantly decreased ($p < 0.001$), while the protein expressions of p53, p62 and caspase-3 were significantly increased ($p = 0.01$, $p < 0.05$ and $p < 0.001$, respectively). Compared with the model group, the protein expressions of beclin, Sirt1 and LC3II in the astragaloside IV 12.16 and 24 μmol L^{-1} group were significantly increased, while the protein expressions of p53, p62 and caspase-3 in each concentration group were significantly decreased ($p = 0.03$ or $p < 0.001$).

Myocardial hypertrophy is a compensatory response to ischemia, hypoxia or pressure overload conditions, mainly manifested as myocardial cell hypertrophy, increased apoptosis, myocardial tissue fibrosis and extracellular deposition of collagen fibers, *etc*. (16). The non-selective *β*-receptor agonist ISO can induce myocardial hypertrophy by stimulating cardiac *β*-receptors and is currently recognized as the main drug for constructing myocardial hypertrophy models (15). Studies have shown that ISO can increase energy metabolism and oxygen free radical production in cardiomyocytes and promote cell apoptosis (13). In this experiment, after H9c2 cells were treated with 100 μmol L^{-1} ISO for 24 hours, it was observed that the viability of H9c2 cells decreased significantly, the cell surface area increased significantly, and the apoptosis rate increased significantly, confirming that ISO could cause hypertrophic damage to H9c2 cells.

Astragalus membranaceus, a plant used in traditional Chinese medicine, is widely used in clinical practice for cardiovascular diseases such as coronary heart disease, arrhythmia and hypertension (17). Relevant studies have shown that astragaloside IV, total saponins and total flavonoids can effectively protect the myocardium by eliminating free radicals and preventing lipid peroxidation (15). The accumulation of ROS can lead to myocardial systolic failure and structural damage, and activate various hypertrophic signal kinases and transcription factors, which are one of the key factors in the occurrence and development of cardiac hypertrophy (18–20). The staining results of TUNEL and Hoechst 33342 in this experiment showed that with the hypertrophy of cardiomyocytes, the apoptosis rate of cardiomyocytes significantly increased, whereas the treatment with astragaloside IV could reduce ISO-induced cardiomyocyte apoptosis, which was further confirmed by the decrease in caspase-3 protein expression (22–22). The results indicated that astragaloside IV could reduce the expression of Bax and p53 in the myocardial hypertrophy model and increase the expression of Bcl-2. All the above results indicate that astragaloside IV can reverse the accumulation of ROS and the decrease of SOD level caused by ISO-induced cardiomyocytes, alleviate cardiomyocyte apoptosis by regulating mitochondrial oxidative stress, and thereby reduce cardiomyocyte hypertrophic injury.

Recent studies have shown that autophagy maintains cardiac function by eliminating damaged organelles and proteins. The loss of autophagy disrupts protein homeostasis and increases intracellular oxidative stress, accelerating the occurrence and development of cardiac hypertrophy and heart failure (23, 24). Relevant *in vivo* experiments have shown

that the reduction of heart-specific autophagy in adulthood can lead to systolic dysfunction, heart failure and cardiac hypertrophy. Other studies have also confirmed that increasing autophagy and reducing apoptosis can alleviate hypertrophic responses and cardiac dysfunction (20). The results of this study indicate that astragaloside IV can inhibit the expression of p62 and increase the total level expressions of beclin and Sirt1, as well as LC3II. The above results indicate that the protective effect of astragaloside IV on myocardial hypertrophy is also related to the activation of autophagy.

CONCLUSIONS

In conclusion, astragaloside IV can enhance the autophagy level of H9c2 cells, eliminate intracellular damaged substances, reduce oxidative stress, and improve mitochondrial function, thereby alleviating cell hypertrophy damage.

Ethics approval. – The study received ethics approval from Xing Yi People's Hospital. There is no sensitive data, and no patients were recruited for this study.

Conflict of interest. – The authors declare no competing interests.

Funding. – This study was funded by the Joint Medical Research Project of Qianxinan Prefecture in 2024 (No. 2024-68).

Author's contribution. – Conceptualisation, Y.L.; investigation, Y.L., Y.X., C.C., and C.P.; statistical analysis, Y.X.; writing, original draft preparation, Y.L.; writing, review and editing, Y.L., Y.X., C.C., C.P., and Y.Z.; supervision, Y.Z. All authors have read and agreed to the published version of the manuscript.

REFERENCE

1. F. Bazgir, J. Nau, S. Nakhaei-Rad, E. Amin, M. J. Wolf, J. J. Saucerman, K. Lorenz and M. R. Ahmadian, The microenvironment of the pathogenesis of cardiac hypertrophy, *Cells* **12** (2023) Article ID 1780 (35 pages); https://doi.org/10.3390/cells12131780
2. Y. Bei, Y. Zhu, M. Wei, M. Yin, L. Li, C. Chen, Z. Huang, X. Liang, J. Gao, J. Yao, P. H. van der Kraak, A. Vink, Z. Lei, Y. Dai, H. Chen, Y. Liang, J. PG Sluijter and J. Xiao, HIPK1 inhibition protects against pathological cardiac hypertrophy by inhibiting the CREB-C/EBPβ axis, *Adv. Sci.* **10**(18) (2023) e2300585 (15 pages); https://doi.org/10.1002/advs.202300585
3. G. Chen, N. An, J. Shen, H. Chen, Y. Chen, J. Sun, Z. Hu, J. Qiu, C. Jin, S. He, L. Mei, Y. Sui, W. Li, P. Chen, X. Guan, M. Chu, Y. Wang, L. Jin, K. Kim, X. Li, W. Cong and X. Wang, Fibroblast growth factor 18 alleviates stress-induced pathological cardiac hypertrophy in male mice, *Nat. Commun.* **14** (2023) Article ID 1235 (18 pages); https://doi.org/10.1038/s41467-023-36895-1
4. L. Zhou, M. Li, Z. Chai, J. Zhang, K. Cao, L. Deng, Y. Liu, C. Jiao, G.-M. Zou, J. Wu and F. Han, Anticancer effects and mechanisms of astragaloside IV, *Oncol. Rep.* **49** (2023) Article ID 5 (15 pages); https://doi.org/10.3892/or.2022.8442
5. E. M. Boorsma, J. M. ter Maaten, K. Damman, W. Dinh, F. Gustafsson, S. Goldsmith, D. Burkhoff, F. Zannad, J. E. Udelson and A. A. Voors, Congestion in heart failure: A contemporary look at physiology, diagnosis and treatment, *Nat. Rev. Cardiol.* **10** (2020) 641–655; https://doi.org/10.1038/s41569-020-0379-7
6. V. Castiglione, A. Aimo, G. Vergaro, L. Saccaro, C. Passino and M. Emdin, Biomarkers for the diagnosis and management of heart failure, *Heart Fail. Rev.* **2** (2022) 625–643; https://doi.org/10.1007/s10741-021-10105-w

7. C. Bonvicini, S. V. Faraone and C. Scassellati, Attention-deficit hyperactivity disorder in adults: A systematic review and meta-analysis of genetic, pharmacogenetic and biochemical studies, *Mol. Psychiatry* **21** (2016) 872–884; https://doi.org/10.1038/mp.2016.74
8. M. G. Crespo-Leiro and E. Barge-Caballero, Advanced heart failure: Definition, epidemiology, and clinical course, *Heart Fail. Clin.* **17**(4) (2021) 533–545; https://doi.org/10.1016/j.hfc.2021.06.002
9. E. La Franca, G. Manno, L. Ajello, G. Di Gesaro, C. Minà, C. Visconti, D. Bellavia, C. Falletta, G. Romano, S. Dell' Oglio, P. Licata, A. Caronia, M. Gallo and F. Clemenza, Physiopathology and diagnosis of congestive heart failure: Consolidated certainties and new perspectives, *Curr. Probl. Cardiol.* **46**(3) (2021) Article ID 100691 (16 pages); https://doi.org/10.1016/j.cpcardiol.2020.100691
10. Y. Gao, X. Su, T. Xue and N. Zhang, The beneficial effects of astragaloside IV on ameliorating diabetic kidney disease, *Biomed. Pharmacother.* **163** (2023) Article ID 114598 (12 pages); https://doi.org/10.1016/j.biopha.2023.114598
11. X. Chen, T. Yang, Y. Zhou, Z. Mei and W. Zhang; Astragaloside IV combined with ligustrazine ameliorates abnormal mitochondrial dynamics via Drp1 SUMO/deSUMOylation in cerebral ischemia-reperfusion injury, *CNS Neurosci. Ther.* **30**(4) (2024) e14725 (18 pages); https://doi.org/10.1111/cns.14725
12. Y. Liang, B. Chen, D. Liang, X. Quan, R. Gu, Z. Meng, H. Gan, Z. Wu, Y. Sun, S. Liu and G. Dou, Pharmacological effects of astragaloside IV: A review, *Molecules* **28**(16) (2023) Article ID 166118 (16 pages); https://doi.org/10.3390/molecules28166118
13. J. Wan, Z. Zhang, C. Wu, S. Tian, Y. Zang, G. Jin, Q. Sun, P. Wang, X. Luan, Y. Yang, X. Zhan, L. L. Ye, D. D. Duan, X. Liu and W. Zhang, Astragaloside IV derivative HHQ16 ameliorates infarction--induced hypertrophy and heart failure through degradation of lncRNA4012/9456, *Sig. Transduct. Target Ther.* **8** (2023) Article ID 414 (16 pages); https://doi.org/10.1038/s41392-023-01660-9
14. J. Wang, X. Pu, H. Zhuang, Z. Guo, M. Wang, H. Yang, C. Li and X. Chang, Astragaloside IV alleviates septic myocardial injury through DUSP1-prohibitin 2 mediated mitochondrial quality control and ER-autophagy, *J. Adv. Res.* **75** (2025) 561–580; https://doi.org/10.1016/j.jare.2024.10.030
15. P. Umapathi, O. O. Mesubi, P. S. Banerjee, N. Abrol, Q. Wang, E. D. Luczak, Y. Wu, J. M. Granger, A.-C. Wei, O. E. Reyes Gaido, L. Florea, C. Conover Talbot, G. W. Hart, N. E. Zachara and M. E. Anderson, Excessive *O*-GlcNAcylation causes heart failure and sudden death, *Circulation* **143**(17) (2021) 1687–1703; https://doi.org/10.1161/CIRCULATIONAHA.120.051911
16. Z. Feng, L. Pan, C. Qiao, Y. Yang, X. Yang and Y. Xie, Cardamonin intervenes in myocardial hypertrophy progression by regulating Usp18, *Phytomedicine* **134** (2024) Article ID 155970 (12 pages); https://doi.org/10.1016/j.phymed.2024.155970
17. E. Dai, X. Guo, J. Wang, Q. Hu, J. Li, Q. Tang, H. Zu, H. Huan, Y. Wang, Y. Gao, G. Hu, W. Li, Z. Liu, Q. Ma, Y. Song, J. Yang, Y. Zhu, S. Huang, Z. Meng, B. Bai, Y. Chen, C. Gao, M. Huang, S. Jin, M. Lu, Z. Xu, Q. Zhang, S. Zheng, Q. Zeng and X. Qi, Investigate of the etiology and prevention status of liver cirrhosis, *Zhonghua Yi Xue Za Zhi*, **12** (2023) 913–919; https://doi.org/10.3760/cma.j.cn112137-20221017-02164
18. S. Kaul, A. Embaby, K. M. Heinhuis, N. S. IJzerman, A. M. Koenen, S. van der Kleij, I. Hofland, H. van Boven, J. Sanders, W. T. A. van der Graaf, R. L. Haas, A. D. R. Huitema, W. J. van Houdt and N. Steeghs, Propranolol monotherapy in angiosarcoma – A window-of-opportunity study (PropAngio), *Eur. J. Cancer* **202** (2024) Article ID 113974 (7 pages); https://doi.org/10.1016/j.ejca.2024.113974
19. D. E. Le, N. J. Alkayed, Z. Cao, N. N. Chattergoon, M. Garcia-Jaramillo, K. Thornburg and S. Kaul, Metabolomics of repetitive myocardial stunning in chronic multivessel coronary artery stenosis: Effect of non-selective and selective β1-receptor blockers, *J. Physiol.* **602**(14) (2024) 3423–3448; https://doi.org/10.1113/JP285720
20. X. Wang, Y. Wang, D. Huang, S. Shi, P. Caixia, Y. Wu, S. Zherui, F. Wang, Z. Wang, Astragaloside IV regulates the ferroptosis signaling pathway via the Nrf2/SLC7A11/GPX4 axis to inhibit PM2.5-

mediated lung injury in mice, *Int. Immunopharmacol.* **112** (2022) Article ID 109186 (12 pages); https://doi.org/10.1016/j.intimp.2022.109186

21. K. Okabayashi, Y. Wakao and T. Narita, Release of secretory immunoglobulin A by submandibular gland via β adrenergic receptor stimulation, *Arch. Oral Biol.* **129** (2021) Article ID 105209 (5 pages); https://doi.org/10.1016/j.archoralbio.2021.105209
22. Y. Q. Tan, H. W. Chen and J. Li, Astragaloside IV: An effective drug for the treatment of cardiovascular diseases, *Drug Des. Devel. Ther.* **14** (2020) 3731–3746; https://doi.org/10.2147/DDDT.S272355
23. W. Tian, P. Zhang, L. Yang, P. Song, J. Zhao, H. Wang, Y. Zhao and L. Cao, Astragaloside IV alleviates doxorubicin-induced cardiotoxicity by inhibiting cardiomyocyte pyroptosis through the SIRT1/NLRP3 pathway, *Am. J. Chin. Med.* **52**(2) (2024) 453–469; https://doi.org/10.1142/S0192415X24500198
24. Y. Su, X. Yin, X. Huang, Q. Guo, M. Ma, L. Guo, Astragaloside IV ameliorates sepsis-induced myocardial dysfunction by regulating NOX4/JNK/BAX pathway, *Life Sci.* **310** (2022) Article ID 121123 (10 pages); https://doi.org/10.1016/j.lfs.2022.121123